

A tensor model for nematic phases of bent-core molecules based on molecular theory

Jie Xu^{1,*}, Fangfu Ye^{2,3} & Pingwen Zhang^{1†}

¹LMAM & School of Mathematical Sciences, Peking University, Beijing 100871, China

²Beijing National Laboratory for Condensed Matter Physics,
Institute of Physics, Chinese Academy of Sciences, Beijing 100190, China

³School of Physical Sciences, University of Chinese Academy of Sciences, Beijing 100094, China

E-mail: rxj_2004@126.com, fye@iphy.ac.cn, pzhang@pku.edu.cn

April 19, 2019

Abstract

We construct a tensor model for nematic phases of bent-core molecules from molecular theory. The form of free energy is determined by molecular symmetry, which includes the couplings and derivatives of a vector and two second-order tensors, with the coefficients determined by molecular parameters. We use the model to study the nematic phases resulted from the hard-core potential, and obtain the phase diagram about the molecular parameters. The tensor model is applicable to other molecules with the same symmetry, which we demonstrate by studying the phase diagram of star molecules.

Keywords: Liquid crystals; Bent-core molecules; Tensor model; Molecular theory; Modulated nematic phases; Twist-bend phase.

1 Introduction

The ability to show complex orientational order has drawn much attention of the liquid crystal community to bent-core molecules. This feature originates from the C_{2v} molecular symmetry that breaks the axisymmetry of a rod-like molecule. The polar and biaxial order is notable in layer or columnar structures [6, 25]. Moreover, bent-core molecules are able to exhibit modulated nematic phases that have constant number density in space but show modulation in orientational distribution. The prediction has been made very early [16, 8]. Later the twist-bend phase has been identified experimentally [22, 9, 21, 18, 3, 5].

The modulated nematic phases have also been discussed theoretically with different models [13, 24, 19, 26, 23]. These models are helpful to understanding the phase behaviours. However, they are presented as macroscopic phenomenological model suitable only for particular phase transitions. In particular, all of these models do not include the biaxial nematic phase that has been confirmed experimentally [14, 1], which is studied separately in

*Current address: Department of Mathematics, Purdue University, West Lafayette, IN 47907, USA

†Corresponding author

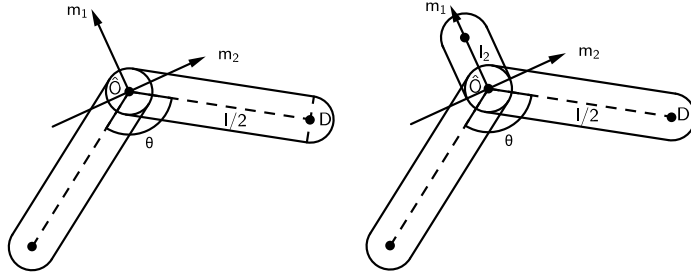


Fig. 1: A bent-core molecule (left) and a star molecule (right).

the literature (see [2] and the references therein). Moreover, the connection between the molecular interaction and the resulting nematic phases, the fundamental problem for liquid crystals, is still not clear from these models. On the other hand, many molecular simulations [4, 17, 12, 7, 20] have also been carried out for bent-core molecules. A recent work [10] use both molecular theory and molecular simulation to study a curved molecule that can exhibit the twist-bend phase. Molecular theory or molecular simulation can, indeed, build connection between molecular interaction and phase behavior, but also with expensive computational cost.

In this work, we construct a tensor model for nematic phases of bent-core molecules from molecular theory. The derivation is based on [28] discussing the order parameters and homogeneous phases, and is an extension of the work [11] for rod-like molecules. The orientation is described by two second-order tensors and a polar vector as in [28]. The model contains derivatives of the tensors that enable us to study modulated nematic phases. The form of free energy is determined by the molecular symmetry, and the coefficients are derived from the hard-core interaction as functions of molecular parameters. The model is presented in a macroscopic form that is much easier to solve than molecular theory, meanwhile retaining the characteristic of microscopic interaction in the coefficients. We use the model to study the nematic phases of bent-core molecules, and find that the uniaxial and biaxial nematic phases, as well as the modulated twist-bend phase are all possible to occur, which cover all the nematic phases found experimentally. We obtain the phase diagram about molecular parameters, showing how the molecular parameters affect the modulation in the twist-bend phases. In addition, we examine the nematic phases of star molecules, a variant of bent-core molecules, to illustrate the effect of the molecular shape on the phase behavior.

The rest of paper is organized as follows. In Sec. 2 we derive the tensor model from molecular theory. The numerical results are presented in Sec. 3. A concluding remark is given in Sec. 4. Some details are given in Appendix.

2 The tensor model

2.1 Notations

We consider bent-core molecules and star molecules, drawn in Fig. 1. A bent-core molecule has two identical arm joint with fixed angle θ . Each arm is generated by inflating each point on a line segment of the length $l/2$ to a sphere of diameter D . A star molecule has a third arm of the length l_2 along the arrowhead direction. Both molecules are regarded

as fully rigid. Thus the position and orientation of a molecule are represented by those of the orthonormal frame $(\hat{O}; \mathbf{m}_1, \mathbf{m}_2, \mathbf{m}_3)$ mounted on it. As shown in Fig. 1, \mathbf{m}_1 points toward the arrowhead direction, and \mathbf{m}_2 is along the connection of the farther ends of two arms. Both molecules have the symmetry plane $\hat{O}\mathbf{m}_1\mathbf{m}_2$ and the twofold rotational symmetry round \mathbf{m}_1 . Denote by $\mathbf{x} \in \mathbb{R}^3$ the position of \hat{O} and by $P \in SO(3)$ the orientation of the frame. The matrix representation of P , which consists of the components of \mathbf{m}_i , can be expressed by Euler angles,

$$P = (\mathbf{m}_1, \mathbf{m}_2, \mathbf{m}_3) = \begin{pmatrix} m_{11} & m_{21} & m_{31} \\ m_{12} & m_{22} & m_{32} \\ m_{13} & m_{23} & m_{33} \end{pmatrix} = \begin{pmatrix} \cos \alpha & -\sin \alpha \cos \gamma & \sin \alpha \sin \gamma \\ \sin \alpha \cos \beta & \cos \alpha \cos \beta \cos \gamma - \sin \beta \sin \gamma & -\cos \alpha \cos \beta \sin \gamma - \sin \beta \cos \gamma \\ \sin \alpha \sin \beta & \cos \alpha \sin \beta \cos \gamma + \cos \beta \sin \gamma & -\cos \alpha \sin \beta \sin \gamma + \cos \beta \cos \gamma \end{pmatrix}. \quad (2.1)$$

The uniform probability measure on $SO(3)$ is given by

$$dP = \frac{1}{8\pi^2} \sin \alpha d\alpha d\beta d\gamma.$$

We can also view \mathbf{m}_i and m_{ij} as functions of P . In what follows, we use the notation $\mathbf{m}_i(P)$ and $m_{ij}(P)$ to represent the \mathbf{m}_i and m_{ij} determined by a certain P .

The summation over repeated indices will be used. The product $\mathbf{m}_1\mathbf{m}_1$ is recognized as tensor product and results in a second-order tensor, while $\mathbf{m}_1 \cdot \mathbf{m}_2$ is the inner product. For second-order tensor Q , we use $|Q|^2 = Q : Q = Q_{ij}Q_{ij}$.

2.2 The derivation of tensor model

Our starting point is the second virial expansion. The free energy includes the entropy and the contribution of pairwise molecular interaction,

$$\frac{F[f]}{k_B T} = \int dP d\mathbf{x} f(\mathbf{x}, P) \log f(\mathbf{x}, P) + \frac{1}{2} \int dP d\mathbf{x} dP' d\mathbf{x}' f(\mathbf{x}, P) G(\mathbf{r}, P, P') f(\mathbf{x}', P'), \quad (2.2)$$

where the energy is measured by $k_B T$, the product of the Boltzmann constant and the temperature, and $\mathbf{r} = \mathbf{x}' - \mathbf{x}$ is the relative position of two molecules. The number density f is a function of the position \mathbf{x} and the orientation P . We define $c(\mathbf{x}) = \int dP f(\mathbf{x}, P)$ as the spatial concentration, and $\rho(\mathbf{x}, P) = f(\mathbf{x}, P)/c(\mathbf{x})$ as the orientational density. They satisfy

$$\int d\mathbf{x} dP f(\mathbf{x}, P) = \int d\mathbf{x} c(\mathbf{x}) \int dP \rho(\mathbf{x}, P) = c_0 V,$$

where V is the volume of the system, and c_0 is the average concentration. The kernel $G(\mathbf{r}, P, P')$ is the Mayer function $G = 1 - \exp(-U/k_B T)$ [15] about the pairwise potential U . In the case of hard-core potential, if two molecules touch, then $U(\mathbf{r}, P, P') = +\infty$, leading to $G(\mathbf{r}, P, P') = 1$; otherwise $U(\mathbf{r}, P, P') = 0$, namely $G(\mathbf{r}, P, P') = 0$.

We will derive the tensor model by expanding the pairwise interaction term in (2.2) about \mathbf{r} and P . After the expansion, we can express the pairwise interaction term by three tensors. Then we minimize the entropy term with the value of these tensors fixed, so that it is also expressed as a functional of three tensors.

2.2.1 Spatial and orientational expansion

First, we do Taylor expansion on $f(\mathbf{x}', P') = f(\mathbf{x} + \mathbf{r}, P')$ with respect to \mathbf{r} , yielding

$$\begin{aligned} \frac{F[f]}{k_B T} &= \int dP d\mathbf{x} f(\mathbf{x}, P) \log f(\mathbf{x}, P) \\ &+ \sum_{k \geq 0} \frac{1}{2k!} \int d\mathbf{x} dP dP' f(\mathbf{x}, P) M^{(k)}(P, P') \nabla^k f(\mathbf{x}, P'), \end{aligned} \quad (2.3)$$

where

$$M^{(k)}(P, P') = \int G(\mathbf{r}, P, P') \underbrace{\mathbf{r} \dots \mathbf{r}}_{k \text{ times}} d\mathbf{r},$$

a k th-order symmetric tensor, is the k th moment of G . For the hard-core interaction, the integration is taken on the region where $G = 1$. By determining this region, we are able to calculate $M^{(k)}$ numerically. The detail is described in Appendix. Because the size of the region is proportional to l^3 , we have $M^{(k)} \propto l^{k+3}$. Similar to rod-like molecules, we will truncate at $M^{(2)}$ since we only examine nematic phases.

Next we describe the expansion of $M^{(k)}(P, P')$. We aim to approximate each component of $M^{(k)}$ as a polynomial of $m_{ij}(P)$ and $m'_{ij} = m_{ij}(P')$, while meeting the symmetric properties. Specifically, we only retain the terms such that the degrees of m_{ij} and m'_{ij} are no more than second order respectively. For instance, we accept $m_{22}^2 m_{22}'^2$, but will discard m_{11}^3 .

Denote the relative orientation as

$$\bar{P} = P^{-1} P' = (p_{ij})_{3 \times 3} = (\mathbf{m}_i \cdot \mathbf{m}'_j), \quad (2.4)$$

where we denote $\mathbf{m}'_i = \mathbf{m}_i(P')$. The following equalities shall be satisfied for molecules with symmetry plane $\hat{O}\mathbf{m}_1\mathbf{m}_2$,

$$G(T\mathbf{r}, TP, TP') = G(\mathbf{r}, P, P'), \quad (2.5)$$

$$G(-\mathbf{r}, P', P) = G(\mathbf{r}, P, P'), \quad (2.6)$$

$$G(-\mathbf{r}, PJ, P'J) = G(\mathbf{r}, P, P') \text{ for } J = \text{diag}(-1, -1, 1). \quad (2.7)$$

The above equalities have been stated in [28]. The meaning of the three equalities is that G is invariant when two molecules rotate together, when two molecules are switched, and when one molecule is reflected about the plane $\hat{O}\mathbf{m}_1\mathbf{m}_2$ of the other molecule.

As the simplest case, we first review the expansion of $M^{(0)}$ discussed in [28]. It also plays an important role in the expansion of $M^{(1)}$ and $M^{(2)}$. It follows from (2.5) that $M^{(0)}$ is a function of the relative orientation \bar{P} . Then from (2.7), we deduce that

$$M^{(0)}(\bar{P}) = M^{(0)}(J\bar{P}J).$$

Note that \bar{P} and $J\bar{P}J$ are the only two elements in SO_3 when $(p_{11}, p_{12}, p_{21}, p_{22})$ is fixed. Hence $M^{(0)}$ is reduced to a function of the above four scalars. And by (2.6), we have

$$M^{(0)}(p_{11}, p_{12}, p_{21}, p_{22}) = M^{(0)}(p_{11}, p_{21}, p_{12}, p_{22}). \quad (2.8)$$

We use a polynomial of p_{11} , p_{12} , p_{21} , p_{22} to approximate $M^{(0)}$, denoted by $\hat{M}^{(0)}$. It shall satisfy (2.8) as well. Furthermore, it has the $\mathbf{m}_2 \rightarrow -\mathbf{m}_2$ and $\mathbf{m}'_2 \rightarrow -\mathbf{m}'_2$ symmetries. Since

$p_{ij} = \mathbf{m}_i \cdot \mathbf{m}'_j$, only the terms where both \mathbf{m}_2 and \mathbf{m}'_2 appear even times can be retained. For example, the term $p_{22} = \mathbf{m}_2 \cdot \mathbf{m}'_2$ will be discarded since both \mathbf{m}_2 and \mathbf{m}'_2 appear one time. Thus we obtain the following quadratic approximation

$$\hat{M}^{(0)} = c_{00} + c_{01}p_{11} + c_{02}p_{11}^2 + c_{03}p_{22}^2 + c_{04}(p_{12}^2 + p_{21}^2). \quad (2.9)$$

The first index of the coefficients c_{0j} is zero, corresponding to the zeroth moment $M^{(0)}$. These coefficients are independent of P and P' .

Now we move on to $M^{(1)}$. Since it is no longer a scalar, an additional step is needed before the polynomial approximation. We write

$$M^{(1)}(P, P') = \tilde{c}_1 \mathbf{m}_1 + \tilde{c}_2 \mathbf{m}_2 + \tilde{c}_3 \mathbf{m}_3. \quad (2.10)$$

To write (2.10) symmetric about \mathbf{m}_i and \mathbf{m}'_i , we express \mathbf{m}_3 by linear combination of \mathbf{m}_1 , \mathbf{m}_2 , \mathbf{m}'_1 and \mathbf{m}'_2 . In general cases, it may cause failure when $\mathbf{m}_3 = \pm \mathbf{m}'_3$. But if the molecule has the symmetry plane $\hat{O}\mathbf{m}_1\mathbf{m}_2$, by (2.7) we have $\tilde{c}_3 = 0$ when $\mathbf{m}_3 = \pm \mathbf{m}'_3$. Thus we can write

$$M^{(1)}(P, P') = \tilde{c}_1 \mathbf{m}_1 + \tilde{c}_2 \mathbf{m}_2 + \tilde{c}_{1'} \mathbf{m}'_1 + \tilde{c}_{2'} \mathbf{m}'_2. \quad (2.11)$$

Although the above representation is not unique, it will not affect us to analyze the symmetric properties of the scalars \tilde{c}_j ($j = 1, 2, 1', 2'$) that are functions of (P, P') , and we will follow the same route of writing down $\hat{M}^{(0)}$ to find polynomial approximations of them. First, they are functions of \bar{P} . Actually, if we substitute (P, P') with (TP, TP') in (2.11), by (2.5), the left-hand side becomes

$$\begin{aligned} M^{(1)}(TP, TP') &= \int \mathbf{r} G(\mathbf{r}, TP, TP') d\mathbf{r} = \int \mathbf{r} G(T^{-1}\mathbf{r}, P, P') d\mathbf{r} \\ &= \int T\mathbf{r} G(\mathbf{r}, P, P') d\mathbf{r} = TM^{(1)}(P, P'). \end{aligned}$$

Since $\mathbf{m}_i(TP) = T\mathbf{m}_i$, the right-hand side of (2.11) becomes

$$\tilde{c}_1 T\mathbf{m}_1 + \tilde{c}_2 T\mathbf{m}_2 + \tilde{c}_{1'} T\mathbf{m}'_1 + \tilde{c}_{2'} T\mathbf{m}'_2.$$

Hence \tilde{c}_j remain invariant. In the same way, we can deduce from (2.7) that \tilde{c}_j are functions of $(p_{11}, p_{12}, p_{21}, p_{22})$. Then by (2.6), we have

$$\tilde{c}_l(p_{11}, p_{12}, p_{21}, p_{22}) = -\tilde{c}_{l'}(p_{11}, p_{21}, p_{12}, p_{22}), \quad l = 1, 2. \quad (2.12)$$

Now we write down the polynomial approximation of \tilde{c}_l and $\tilde{c}_{l'}$ with attention to the $\mathbf{m}_2 \rightarrow -\mathbf{m}_2$ and $\mathbf{m}'_2 \rightarrow -\mathbf{m}'_2$ symmetries. The degree of polynomial is chosen such that both \mathbf{m}_i and \mathbf{m}'_i are truncated at second order in (2.11). For example, the term $p_{21}\mathbf{m}_2$ can be rewritten as $(\mathbf{m}_2 \cdot \mathbf{m}'_1)\mathbf{m}_2$, in which the order of \mathbf{m}_2 is two. The polynomial approximations are written as

$$\begin{aligned} \tilde{c}_1 &= -c_{10} - c_{11}p_{11}, & \tilde{c}_{1'} &= c_{10} + c_{11}p_{11}, \\ \tilde{c}_2 &= -c_{12}p_{21}, & \tilde{c}_{2'} &= c_{12}p_{12}, \end{aligned}$$

where the first index of c_{1j} becomes one since they come from $M^{(1)}$. The coefficients c_{1j} are independent of P and P' .

The expansion of $M^{(2)}$ follows the same way as $M^{(1)}$. We can write

$$\begin{aligned}
M^{(2)}(P, P') = & \tilde{c}_{00'} I + \sum_{l_1, l_2=1,2} \tilde{c}_{l_1 l_2} \mathbf{m}_{l_1} \mathbf{m}_{l_2} + \sum_{l'_1, l'_2=1',2'} \tilde{c}_{l'_1 l'_2} \mathbf{m}'_{l'_1} \mathbf{m}'_{l'_2} \\
& + \sum_{l=1,2, l'=1',2'} \tilde{c}_{ll'} (\mathbf{m}_l \mathbf{m}'_{l'} + \mathbf{m}'_{l'} \mathbf{m}_l),
\end{aligned} \tag{2.13}$$

where we require

$$\tilde{c}_{l_1 l_2} = \tilde{c}_{l_2 l_1}, \quad \tilde{c}_{l'_1 l'_2} = \tilde{c}_{l'_2 l'_1}$$

because $M^{(2)}$ is symmetric. Here we include the identity matrix I because its components are zeroth-degree polynomials. Also we are able to exclude \mathbf{m}_3 and \mathbf{m}'_3 for the symmetry plane $\hat{O}\mathbf{m}_1\mathbf{m}_2$. Analogous to $M^{(1)}$, we can deduce from (2.5) and (2.7) that $\tilde{c}_{j_1 j_2}$ are functions of $(p_{11}, p_{12}, p_{21}, p_{22})$. Then by (2.6), we have

$$\begin{aligned}
\tilde{c}_{l_1 l_2}(p_{11}, p_{12}, p_{21}, p_{22}) &= \tilde{c}_{l'_1 l'_2}(p_{11}, p_{21}, p_{12}, p_{22}), \\
\tilde{c}_{l_1 l'_2}(p_{11}, p_{12}, p_{21}, p_{22}) &= \tilde{c}_{l_2 l'_1}(p_{11}, p_{21}, p_{12}, p_{22}).
\end{aligned} \tag{2.14}$$

By noting the $\mathbf{m}_2 \rightarrow -\mathbf{m}_2$ and $\mathbf{m}'_2 \rightarrow -\mathbf{m}'_2$ symmetries, and keeping the truncation at the second order, the polynomial approximations of $\tilde{c}_{j_1 j_2}$ are written as follows,

$$\begin{aligned}
\tilde{c}_{00'} &= -c_{20} - c_{21}p_{11} - c_{22}p_{11}^2 - c_{23}p_{22}^2 - c_{24}(p_{12}^2 + p_{21}^2), \\
\tilde{c}_{11} &= \tilde{c}_{1'1'} = -c_{25}, \\
\tilde{c}_{22} &= \tilde{c}_{2'2'} = -c_{26}, \\
\tilde{c}_{11'} &= \tilde{c}_{1'1} = -c_{27} - c_{28}p_{11}, \\
\tilde{c}_{22'} &= \tilde{c}_{2'2} = c_{29}p_{22}, \\
\tilde{c}_{12} &= \tilde{c}_{21} = \tilde{c}_{1'2'} = \tilde{c}_{2'1'} = 0, \\
\tilde{c}_{12'} &= -c_{2,10}p_{12}, \quad \tilde{c}_{21'} = -c_{2,10}p_{21}.
\end{aligned}$$

Just as the notation for M^0 and $M^{(1)}$, the first index of c_{2j} is two. Again the coefficients c_{2j} do not depend on P and P' .

Summarizing the above derivation, we obtain the expansion of $M^{(0)}$, $M^{(1)}$, $M^{(2)}$, denoted by $\hat{M}^{(0)}$, $\hat{M}^{(1)}$, $\hat{M}^{(2)}$,

$$\begin{aligned}
\hat{M}^{(0)} &= c_{00} + c_{01}p_{11} + c_{02}p_{11}^2 + c_{03}p_{22}^2 + c_{04}(p_{12}^2 + p_{21}^2), \\
\hat{M}^{(1)} &= (-c_{10} - c_{11}p_{11})(\mathbf{m}_1 - \mathbf{m}'_1) - c_{12}(p_{21}\mathbf{m}_2 - p_{12}\mathbf{m}'_2), \\
\hat{M}^{(2)} &= -(c_{20} + c_{21}p_{11} + c_{22}p_{11}^2 + c_{23}p_{22}^2 + c_{24}(p_{12}^2 + p_{21}^2))I \\
&\quad - c_{25}(\mathbf{m}_1\mathbf{m}_1 + \mathbf{m}'_1\mathbf{m}'_1) - c_{26}(\mathbf{m}_2\mathbf{m}_2 + \mathbf{m}'_2\mathbf{m}'_2) \\
&\quad - (c_{27} + c_{28}p_{11})(\mathbf{m}_1\mathbf{m}'_1 + \mathbf{m}'_1\mathbf{m}_1) \\
&\quad - c_{29}p_{22}(\mathbf{m}_2\mathbf{m}'_2 + \mathbf{m}'_2\mathbf{m}_2) \\
&\quad - c_{2,10} [p_{12}(\mathbf{m}_1\mathbf{m}'_2 + \mathbf{m}'_2\mathbf{m}_1) + p_{21}(\mathbf{m}_2\mathbf{m}'_1 + \mathbf{m}'_1\mathbf{m}_2)].
\end{aligned} \tag{2.15}$$

Define

$$\mathbf{p} = \langle \mathbf{m}_1 \rangle, \quad Q_1 = \langle \mathbf{m}_1 \mathbf{m}_1 \rangle, \quad Q_2 = \langle \mathbf{m}_2 \mathbf{m}_2 \rangle, \tag{2.16}$$

where $\langle \cdot \rangle = \int dP(\cdot)\rho(P)$ denotes the average about the orientational density ρ . When we substitute $M^{(k)}$ with $\hat{M}^{(k)}$ in (2.15), we obtain some terms expressed in \mathbf{p} , Q_1 , Q_2 . For example, the term p_{12}^2 in $\hat{M}^{(0)}$ generates the term $cQ_1 : cQ_2$,

$$\begin{aligned} & \int d\mathbf{x} dP dP' p_{12}^2 \cdot f(\mathbf{x}, P) f(\mathbf{x}, P') \\ &= \int d\mathbf{x} \left(c(\mathbf{x}) \int dP m_{1i} m_{1j} \rho(\mathbf{x}, P) \right) \left(c(\mathbf{x}) \int dP' m'_{2i} m'_{2j} \rho(\mathbf{x}, P') \right) \\ &= \int d\mathbf{x} (c(\mathbf{x}) \langle m_{1i} m_{1j} \rangle) (c(\mathbf{x}) \langle m_{2i} m_{2j} \rangle). \end{aligned} \quad (2.17)$$

We will write down all the terms afterwards in (2.23).

2.2.2 The entropy term

The entropy term can be rewritten as

$$\int d\mathbf{x} dP c \rho (\log c + \log \rho) = \int d\mathbf{x} c \log c + \int d\mathbf{x} \left(c(\mathbf{x}) \int dP \rho \log \rho \right).$$

By minimizing $\int dP \rho \log \rho$ with the values of \mathbf{p} , Q_1 and Q_2 fixed, we obtain the Boltzmann distribution,

$$\rho = \frac{1}{Z} \exp(\mathbf{p} \cdot \mathbf{m}_1 + B_1 : \mathbf{m}_1 \mathbf{m}_1 + B_2 : \mathbf{m}_2 \mathbf{m}_2), \quad (2.18)$$

where Z is the normalization factor,

$$Z = \int dP \exp(\mathbf{p} \cdot \mathbf{m}_1 + B_1 : \mathbf{m}_1 \mathbf{m}_1 + B_2 : \mathbf{m}_2 \mathbf{m}_2). \quad (2.19)$$

The vector \mathbf{b} and the symmetric matrices B_1 and B_2 are Lagrange multipliers that make the averages defined in (2.16) be equal to the given values.

We require that Q_1 and Q_2 share an eigenframe and that \mathbf{p} is their eigenvector. This approximation comes from a theoretical result for homogeneous phases [29]. In other words, there exists a $T = (\mathbf{n}_1, \mathbf{n}_2, \mathbf{n}_3) \in SO_3$ such that

$$\mathbf{p} = s\mathbf{n}_1, \quad Q_1 = q_{11}\mathbf{n}_1\mathbf{n}_1 + q_{12}\mathbf{n}_2\mathbf{n}_2 + q_{13}\mathbf{n}_3\mathbf{n}_3, \quad Q_2 = q_{21}\mathbf{n}_1\mathbf{n}_1 + q_{22}\mathbf{n}_2\mathbf{n}_2 + q_{23}\mathbf{n}_3\mathbf{n}_3, \quad (2.20)$$

with $(\mathbf{n}_1, \mathbf{n}_2, \mathbf{n}_3) = (\mathbf{e}_1, \mathbf{e}_2, \mathbf{e}_3)T$ and $q_{i3} = 1 - q_{i1} - q_{i2}$. The eigenvalues shall satisfy

$$\begin{aligned} & q_{ij} > 0, s^2 < q_{11}, \\ & q_{11} + q_{12}, q_{11} + q_{21}, q_{12} + q_{22}, q_{21} + q_{22} < 1, \\ & q_{11} + q_{12} + q_{21} + q_{22} > 1. \end{aligned} \quad (2.21)$$

Furthermore, for any (s, q_{ij}) satisfying the above constraints, there exists a unique (\mathbf{b}, B_1, B_2) of the form

$$\mathbf{b} = T(b_1, 0, 0)^T, B_1 = T \text{diag}(b_{11}, b_{12}, 0) T^T, B_2 = T \text{diag}(b_{21}, b_{22}, 0) T^T, \quad (2.22)$$

such that the moments of the corresponding Boltzmann distribution are (\mathbf{p}, Q_1, Q_2) . The proof is left to Appendix.

2.2.3 The free energy

From (2.3), (2.15), (2.18) and integration by parts, and assuming that $c(\mathbf{x}) = c_0$ is constant, the tensor model is written as follows,

$$\begin{aligned} \frac{F[Q_1, Q_2, \mathbf{p}]}{k_B T} = \int d\mathbf{x} \Big\{ & c(\mathbf{b} \cdot \mathbf{p} + B_1 : Q_1 + B_2 : Q_2 - \log Z) \\ & + \frac{c^2}{2} (c_{01} |\mathbf{p}|^2 + c_{02} |Q_1|^2 + c_{03} |Q_2|^2 + 2c_{04} Q_1 : Q_2) \\ & + c^2 (c_{11} p_i \partial_i Q_{1ij} + c_{12} p_j \partial_i Q_{2ij}) \\ & + \frac{c^2}{4} [c_{21} |\nabla \mathbf{p}|^2 + c_{22} |\nabla Q_1|^2 + c_{23} |\nabla Q_2|^2 + 2c_{24} \partial_i Q_{1jk} \partial_i Q_{2jk} \\ & + 2c_{27} \partial_i p_i \partial_j p_j + 2c_{28} \partial_i Q_{1ik} \partial_j Q_{1jk} \\ & + 2c_{29} \partial_i Q_{2ik} \partial_j Q_{2jk} + 4c_{2,10} \partial_i Q_{1ik} \partial_j Q_{2jk}] \Big\}, \end{aligned} \quad (2.23)$$

where the components of \mathbf{p} and Q_k are denoted as p_i and Q_{kij} . The first line comes from the entropy term. The second line comes from $\hat{M}^{(0)}$. The third line comes from $\hat{M}^{(1)}$, referred to as first-order elastic energy. The rest terms come from $\hat{M}^{(2)}$, referred to as second-order elastic energy.

2.3 The coefficients

Now we describe how to calculate the coefficients in (2.23). Note that $M^{(k)}$ is determined by molecular parameters, and the coefficients come from its approximation $\hat{M}^{(k)}$. Hence we minimize the distance between $\hat{M}^{(k)}$ and $M^{(k)}$, defined as

$$\int_{SO_3} dP dP' \|M^{(k)}(P, P'; l, D, \theta) - \hat{M}^{(k)}(P, P'; \{c_{kj}\})\|_F^2, \quad (2.24)$$

where $\|\cdot\|_F$ is the Frobenius norm $\|M\|_F^2 = \sum_{i_1 \dots i_k} |M_{i_1 \dots i_k}|^2$. By solving this linear least-square problem, we can express c_{kj} as functions of the molecular parameters l , D and θ . Furthermore, we have $c_{kj} \propto l^{k+3}$ because $M^{(k)}$ has the same scaling. Therefore, we can further nondimensionalize the model by the substitution $\bar{\mathbf{x}} = \mathbf{x}/l$, $\bar{c} = cl^3$, $\bar{c}_{kj} = c_{kj}/l^{k+3}$. Now \bar{c}_{kj} become functions of two dimensionless parameters $\eta = D/l$ and θ . For star molecules, $\hat{M}^{(k)}$ also depends on l_2 , thus \bar{c}_{kj} are also functions of l_2/l . For convenience, we still express these dimensionless quantities by the original notations.

The second-order elastic energy shall be positive definite to ensure the lower-boundedness of the free energy. This can be guaranteed if the following inequalities hold,

$$\begin{aligned} c_{21}, c_{22}, c_{23}, 2c_{27} + c_{21}, 2c_{28} + c_{22}, 2c_{29} + c_{23} &\geq 0, \\ c_{24}^2 &\leq c_{22}c_{23}, \\ (2c_{2,10} + c_{24})^2 &\leq (2c_{28} + c_{22})(2c_{29} + c_{23}). \end{aligned} \quad (2.25)$$

These inequalities can be easily observed if we rewrite the second-order elastic energy as follows,

$$\frac{1}{4} [c_{21} |\partial_i p_j|^2 + 2c_{27} (\partial_i p_i)^2 + \frac{1}{2} c_{22} |\partial_i Q_{1jk} - \partial_j Q_{1ik}|^2$$

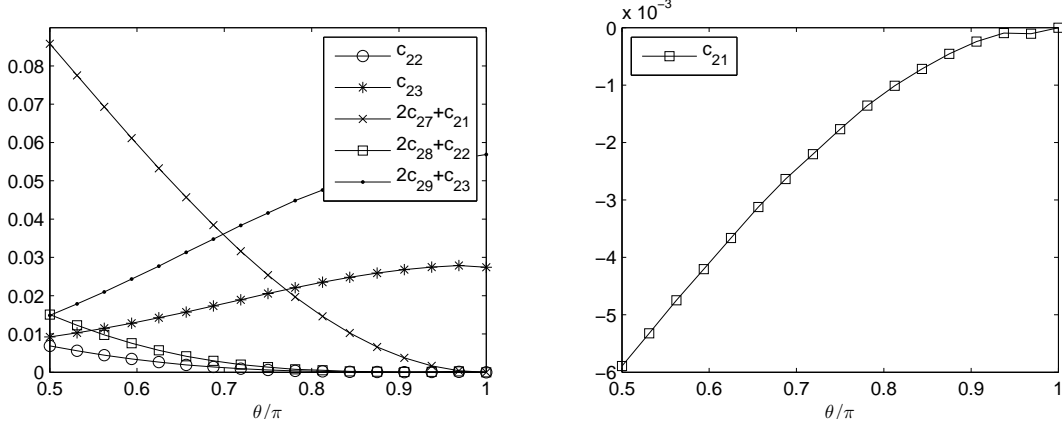


Fig. 2: The coefficients c_{2j} in the second-order elastic energy for bent-core molecules, measured in the unit $(l/2)^5$, as functions of the bending angle θ when $\eta = 1/40$.

$$\begin{aligned}
& + \frac{1}{2}c_{23}|\partial_i Q_{2jk} - \partial_j Q_{2ik}|^2 + c_{24}(\partial_i Q_{1jk} - \partial_j Q_{1ik})(\partial_i Q_{2jk} - \partial_j Q_{2ik}) \\
& + (2c_{28} + c_{22})|\partial_i Q_{1ik}|^2 + (2c_{29} + c_{23})|\partial_i Q_{2ik}|^2 + 2(2c_{2,10} + c_{24})\partial_i Q_{1ik}\partial_j(Q_{2jk})].
\end{aligned}$$

Here we have done some integrations by parts, discarded the boundary terms by adopting periodic boundary conditions, and used the equality

$$\partial_i a_j \partial_i b_j - \partial_i a_j \partial_j b_i = \frac{1}{2}(\partial_i a_j - \partial_j a_i)(\partial_i b_j - \partial_j b_i).$$

Moreover, if $(2c_{2,10} + c_{24})^2 < (2c_{28} + c_{22})(2c_{29} + c_{23})$ or $c_{21} > 0$, it controls the first-order elastic energy. For example,

$$\begin{aligned}
& (2c_{28} + c_{22})|\partial_i Q_{1ik}|^2 + (2c_{29} + c_{23})|\partial_i Q_{2ik}|^2 + 2(2c_{2,10} + c_{24})\partial_i Q_{1ik}\partial_j(Q_{2jk}) \\
& - 4\partial_i p_j(c_{11}Q_{1ij} + c_{12}Q_{2ij}) \geq -C|\mathbf{p}|^2
\end{aligned}$$

for C large enough, and the right-hand side is bounded from below since $|\mathbf{p}| < 1$.

Now we examine whether the coefficients calculated from (2.24) satisfy these conditions. We find that all of the inequalities hold strictly except $c_{21} < 0$ for both bent-core molecules and star molecules. The coefficients of bent-core molecules are plotted in Fig. 2.

The signs of coefficients reflect different modulation mechanism. The term $c_{21}|\nabla \mathbf{p}|^2$ can be stabilized if we truncate up to $M^{(4)}$. In fact, we write down the polynomial approximation $\hat{M}^{(4)}$ following the procedure described above, calculate the coefficients by (2.24), and find that the coefficient $c_{41} > 0$ for the corresponding term $c_{41}|\nabla^2 \mathbf{p}|^2$. The pair $c_{21}|\nabla \mathbf{p}|^2 + c_{41}|\nabla^2 \mathbf{p}|^2$ describes the tendency of independent modulation of \mathbf{p} without coupling to Q_1 and Q_2 . We can see this by taking the plane wave $\phi = \exp(i\mathbf{k} \cdot \mathbf{x})$ into the energy

$$\int d\mathbf{x} |\nabla^2 \phi|^2 + 2K|\nabla \phi|^2 = (|\mathbf{k}|^4 + 2K|\mathbf{k}|^2)|\phi|^2.$$

If $K \geq 0$, the preferred frequency is $\mathbf{k} = 0$; if $K < 0$, the preferred frequency becomes $|\mathbf{k}| = \sqrt{-K} > 0$. On the contrary, the quadratic terms about ∇Q_1 and ∇Q_2 are positive,

indicating that Q_1 and Q_2 do not tend to show independent modulation, but may show modulation coupled with \mathbf{p} through the terms $p_i \partial_j Q_{\sigma ij}$. Currently, we choose not to include the independent modulation of \mathbf{p} as an approximation, and discard the term $c_{21} |\nabla \mathbf{p}|^2$ to avoid lower unboundedness of the energy.

When we consider molecules with other shapes or interactions and calculate the coefficients from (2.24), we may obtain signs of the coefficients different from the above. If this is the case, it indicates that the molecular interaction induces different modulation mechanism, and we need to do a different truncation in accordance with the mechanism.

3 Results and discussion

We examine the phases where inhomogeneity occurs only in the x -direction. To find modulated phases, we need to minimize the free energy density under the periodic boundary condition about the tensors and the period length L ,

$$\min_{\mathbf{p}(x), Q_1(x), Q_2(x), L} \frac{F[\mathbf{p}(x), Q_1(x), Q_2(x)]}{L}.$$

3.1 Numerical methods

We use finite volume method to discretize the free energy. Generally speaking, in $[x_k, x_{k+1}]$, a function $g(x)$ is approximated by $\frac{1}{2}(g(x_k) + g(x_{k+1}))$, and its derivative is approximated by $(g(x_{k+1}) - g(x_k))/(x_{k+1} - x_k)$. For example, the term

$$\int_{x_k}^{x_{k+1}} dx p_i \frac{d}{dx} Q_{1,1i}$$

is approximated by

$$(x_{k+1} - x_k) \cdot \frac{p_i(x_{k+1}) + p_i(x_k)}{2} \cdot \frac{Q_{1,1i}(x_k) - Q_{1,1i}(x_{k+1})}{x_{k+1} - x_k}.$$

A single period is discretized using 32 points. The tensors are represented by their eigenvalues and co-owned eigenframe $T(x)$ that is represented by the Euler angles $(\alpha(x), \beta(x), \gamma(x))$ by (2.1),

$$\begin{aligned} \mathbf{p}(x) &= T(x)(s(x), 0, 0)^T, \\ Q_1(x) &= T(x) \text{diag}(q_{11}(x), q_{12}(x), q_{13}(x)) T(x)^T, \\ Q_2(x) &= T(x) \text{diag}(q_{21}(x), q_{22}(x), q_{23}(x)) T(x)^T. \end{aligned}$$

The eigenvalues are calculated from (b_1, b_{ij}) using (2.18) and (2.22). We will use $(b_1(x), b_{ij}(x))$ and the Euler angles as the basic variables.

The derivatives of the free energy about the eigenvalues are given by

$$\frac{\partial F}{\partial q_{ij}(x)} = b_{ij}(x) + \frac{\partial F_r}{\partial q_{ij}(x)}. \quad (3.1)$$

Here F_r stands for the part of free energy from the pairwise interaction, and the derivatives of the entropy term are calculated by (B.3). The derivatives about the Euler angles are given by

$$\frac{\partial F}{\partial \alpha(x)} = \frac{\partial F_r}{\partial \alpha(x)},$$

since the entropy term is independent of $T(x)$. We use the following stationary point iteration:

$$b_{ij}^{(k+1)}(x) = b_{ij}^{(k)}(x) - \lambda \frac{\partial F}{\partial q_{ij}^{(k)}(x)} = (1 - \lambda) b_{ij}^{(k)}(x) - \lambda \frac{\partial F_r}{\partial q_{ij}^{(k)}(x)}, \quad (3.2)$$

$$\alpha^{(k+1)}(x) = \alpha^{(k)}(x) - \mu \frac{\partial F_r}{\partial \alpha^{(k)}(x)}. \quad (3.3)$$

The iteration is along a descending direction of the free energy (see (B.6)).

The free energy density may have several local minima. Various initial guesses are adopted to obtain as many metastable phases as possible, including but not limited to all the phases presented in the current work. Then we compare free energy density of each metastable phase, and label the minimal one as the stable phase. Many phases that can be stable under other phenomenological coefficients are found unstable or only metastable under coefficients derived from hard-core potential. These phases will be presented in another work [27].

3.2 The phase diagram

We first list the phases that appear in the phase diagram. Define $Q_3 = \langle \mathbf{m}_3 \mathbf{m}_3 \rangle = I - Q_1 - Q_2$ and denote its eigenvalues as q_{3j} . Because T is the eigenframe shared by Q_1 and Q_2 , it is also the eigenframe of Q_3 . For the phases discussed here, we can do permutation such that $q_{ii} \geq q_{ij}$, and assume this in the following. It should be noted that for homogeneous phases, the free energy is independent of the eigenframe T .

- Isotropic phase (I): $s = q_{ij} = 0$.
- Uniaxial nematic phase (N_i): homogeneous with $s = 0$, further classified by the relation of eigenvalues. In the N_2 phase we have $q_{22} > 1/3 > q_{12}, q_{32}$ and $q_{j1} = q_{j3}$. In the N_3 phase we have $q_{33} > 1/3 > q_{13}, q_{23}$ and $q_{j1} = q_{j2}$. The above relations of eigenvalues indicate that in the N_i phase, \mathbf{m}_i aligns near $\pm \mathbf{n}_i$, and the other two \mathbf{m}_j align near the plane perpendicular to \mathbf{n}_i .
- Biaxial nematic phase (B): homogeneous with $q_{ii} > q_{ij}$, indicating that \mathbf{m}_i is preferably along $\pm \mathbf{n}_i$.
- Twist-bend phase (N_{tb}): the eigenvalues s and q_{ij} are constant with $s \neq 0$ and $q_{ii} > q_{ij}$, while $T(x)$ shows the modulation

$$T(x) = (\mathbf{n}_1, \mathbf{n}_2, \mathbf{n}_3) = \begin{pmatrix} 0 & -\cos \gamma & \sin \gamma \\ \cos \frac{\pm 2\pi x}{L} & -\sin \gamma \sin \frac{\pm 2\pi x}{L} & -\cos \gamma \sin \frac{\pm 2\pi x}{L} \\ \sin \frac{\pm 2\pi x}{L} & \sin \gamma \cos \frac{\pm 2\pi x}{L} & \cos \gamma \cos \frac{\pm 2\pi x}{L} \end{pmatrix}, \quad (3.4)$$

where the modulation of \mathbf{n}_2 and \mathbf{n}_3 is identical to the earlier prediction [8]. The above equation indicates that \mathbf{n}_1 rotates on a circle, and that \mathbf{n}_2 rotates on a conical surface.

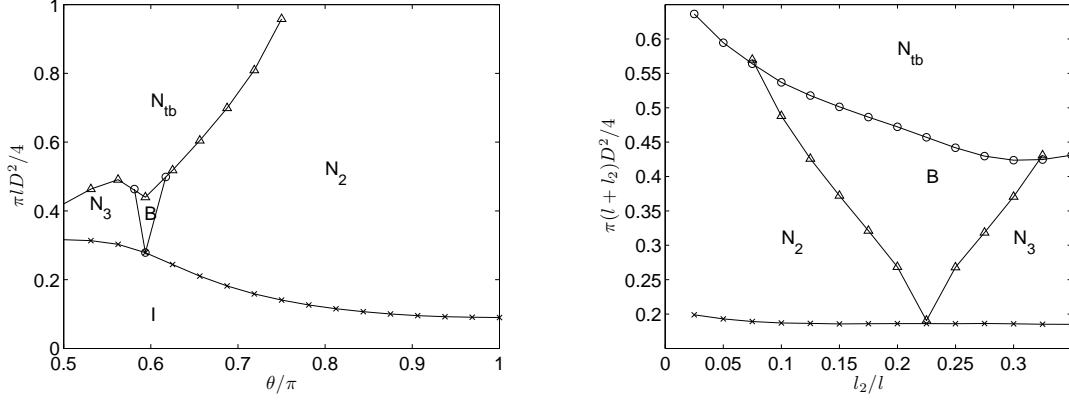


Fig. 3: Left: phase diagram of bent-core molecules with $\eta = D/l = 1/40$. Right: phase diagram of star molecules with $\theta = 2\pi/3$, $\eta = 1/40$.

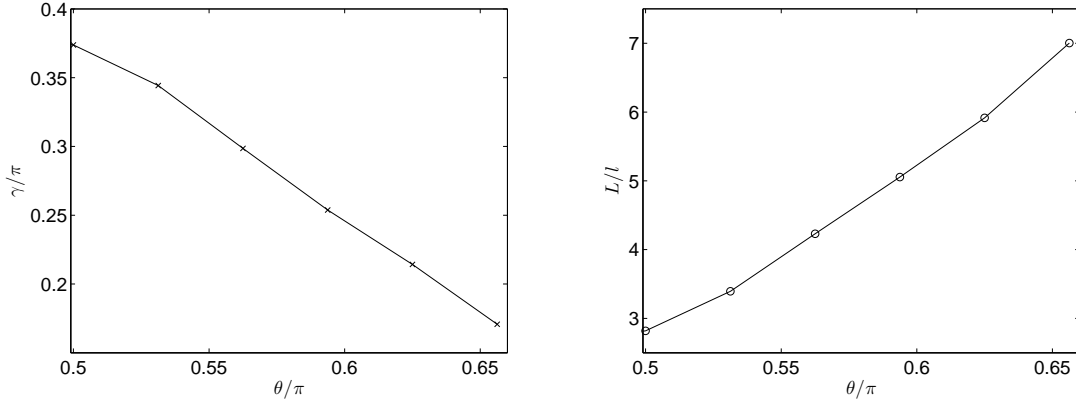


Fig. 4: The conical angle γ and period length L as functions of the bending angle θ when $\pi l D^2/4 = 0.7$.

Thus the Euler angle γ here becomes the conical angle. The sign before $2\pi x$ represents whether T is rotated left- or right-handed. The two cases share the same free energy density.

Although we only examine one-dimensional modulated phases, these phases have covered all the phases found experimentally.

The phase diagram of bent-core molecules is given in Fig. 3 (left), where we fix $\eta = 1/40$, and use the volume fraction $\pi l D^2 c/4$ to express the concentration. It shows that I occurs at low volume fraction, and homogeneous nematic phases emerge when it becomes higher. As the bending angle θ decreases from π , it shows successively N_2 , B and N_3 . When the volume fraction further grows, the N_{tb} phase occurs if the bending angle θ is far from π . We also plot the conical angle γ and period length L as a function of θ at $\pi l D^2 c/4 = 0.7$ (Fig. 4). We observe that as θ increases, γ decreases while L increases.

Next we study the role of the third arm for star molecules. The phase diagram is presented in Fig. 3 (right). Here we fix the bending angle $\theta = 2\pi/3$ and focus on the length of the third

arm l_2/l . Now the volume fraction becomes $\pi(l + l_2)D^2c/4$. The nematic phases are among those we mentioned above, and are sensitive to l_2 . While the transition volume fraction to homogeneous nematic phases is almost unchanged, the phase is altered from N_2 to B and to N_3 when l_2 increases. The transition volume fraction to N_{tb} is substantially lowered as l_2 grows.

For bent-core molecules, phase diagram about molecular parameters including modulated nematic phases has not been given in existing theoretical models. Moreover, in these models that focus on modulated phase, only one director \mathbf{n} , or one second-order tensor Q is included, leading to the absence of the biaxial phase B . Phase diagram about molecular parameters can only be found in preceding molecular simulations [4, 17, 12, 7, 20]. In these works the molecules studied are thick with $\eta \approx 1/5 \sim 1/10$, and they did not find the N_{tb} phase. The results in [10] indicate that curved structure can make N_{tb} easier to occur. Our results suggest that thin molecules might have the same effect.

4 Conclusion

A tensor model is constructed based on molecular theory for nematic phases of bent-core molecules. The free energy is suitable for molecules with the C_{2v} symmetry, with the coefficients derived from molecular interaction. We use the model to study the nematic phases of bent-core molecules and their analog, star molecules, with the hard-core potential. We obtain the phase diagram about the molecular parameters, including all the nematic phases found experimentally. Provided that the molecular symmetry is preserved, the tensor model is able to study molecules with arbitrary shape and interactions. Hence we aim to apply this model to studying nematic phases of various molecules. We are also interested in two- and three-dimensional modulated phases that can be described by the model.

A The computation of $M^{(k)}$

We describe how to compute $M^{(k)}$ for bent-core molecules. It works exactly the same way for star molecules.

Fix the orientation of a pair of molecules. Denote by W_{ij} the region such that when the relative position $\mathbf{r} \in W_{ij}$, the i th arm of one molecule and the j th arm of the other touch. Then the region where two molecules touch, denoted by W , is the union of four W_{ij} . Each W_{ij} is a spheroparallelogram, obtained by inflating each point in a parallelogram to a sphere. One of the W_{ij} is drawn in Fig. 5 (left). All the four W_{ij} contain \hat{O} , since four arms share the point \hat{O} when $\mathbf{r} = 0$.

Denote

$$s_{ij}(\mathbf{n}) = \max_{t\mathbf{n} \in W_{ij}} t.$$

Then

$$\max_{t\mathbf{n} \in W} t \triangleq s(\mathbf{n}) = \max_{i,j=1,2} s_{ij}(\mathbf{n}).$$

For any vector \mathbf{n} , the whole segment $t\mathbf{n}$ ($t \in [0, s(\mathbf{n})]$) lies within W , because W_{ij} are convex. Hence we can express $M^{(k)}$ by an integral in spherical coordinates, which we utilize for

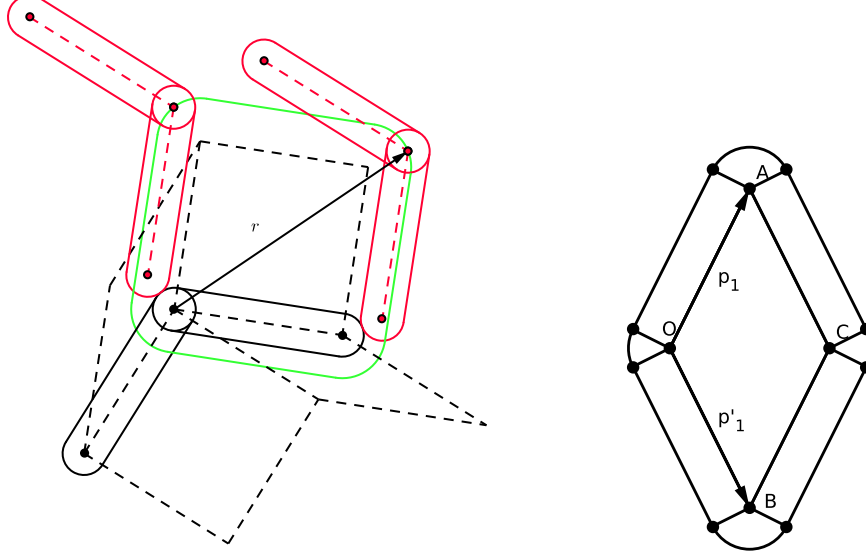


Fig. 5: Left: the region W , consisting of four spheroparallelograms, whose skeleton parallelograms are drawn in dashed line. Right: the intersection of a spheroparallelogram with the plane $z = 0$ where the parallelogram lies in.

numerical calculation,

$$\begin{aligned}
 M^{(k)}(P, P') &= \int_W \underbrace{\mathbf{r} \dots \mathbf{r}}_{k \text{ times}} d\mathbf{r} = \int_{S^2} \underbrace{\mathbf{n} \dots \mathbf{n}}_{k \text{ times}} d\mathbf{n} \int_0^{s(\mathbf{n})} r^{k+2} dr \\
 &= \int_{S^2} \frac{1}{k+3} s(\mathbf{n})^{k+3} \underbrace{\mathbf{n} \dots \mathbf{n}}_{k \text{ times}} d\mathbf{n}.
 \end{aligned} \tag{A.1}$$

Now it remains to compute s_{ij} . Place the parallelogram in the plane $z = 0$. Denote by R the intersection point of the ray $t\mathbf{n}$ ($t \geq 0$) and the boundary of the spheroparallelogram. The boundary of a spheroparallelogram consists of two planes $z = \pm D$, four cylindrical surfaces at four edges, and four spherical surfaces at four vertices. We need to determine where R lies, for which the procedure below is followed:

- Compute the intersection point of the ray $t\mathbf{n}$ and the plane $z = \pm D$. Then examine whether its projection on the plane $z = 0$ lies in the parallelogram $OACB$, drawn in Fig. 5 (right). If it does, the R lies on the flat surface of the spheroparallelogram.
- Determine whether the ray $t\mathbf{n}$ intersects with any of the spheres on the corner. If yes, compute the farthest intersection point and examine its projection on the plane $z = 0$. If it lies in the corresponding sector (located at the corners in Fig. 5), R lies on the spherical surface of the spheroparallelogram.
- Now we know that R lies on the cylindrical surface of the spheroparallelogram, and it is easy to distinguish which cylinder it locates.

B The properties of the Boltzmann distribution

B.1 The existence of the Lagrange multiplier

Let

$$\mathcal{A} = \{(s, q_{ij}) | \rho : SO_3 \rightarrow \mathbb{R}^+, \int d\nu \rho = 1, s = \int d\nu \rho m_{11}, q_{ij} = \int d\nu \rho m_{ij}^2, i, j = 1, 2\}.$$

Theorem B.1. *Each $(s, q_{ij}) \in \mathcal{A}$ is subject to the constraints in (2.21). For any (s, q_{ij}) satisfying (2.21), there exists a unique solution to the minimization problem*

$$\begin{aligned} & \inf_{SO_3} \int d\nu \rho(P) \log \rho(P), \\ \text{s.t. } & \int d\nu \rho(P) = 1, \\ & \int d\nu \mathbf{m}_1 \rho(P) = (s, 0, 0)^T, \\ & \int d\nu \mathbf{m}_1 \mathbf{m}_1 \rho(P) = \text{diag}(q_{11}, q_{12}, 1 - q_{11} - q_{12}), \\ & \int d\nu \mathbf{m}_2 \mathbf{m}_2 \rho(P) = \text{diag}(q_{21}, q_{22}, 1 - q_{21} - q_{22}). \end{aligned}$$

The solution takes the form

$$\rho(P) = \frac{1}{Z} \exp \left(b_1 m_{11} + \sum_{i,j=1,2} b_{ij} m_{ij}^2 \right),$$

where

$$Z = \int d\nu \exp \left(b_1 m_{11} + \sum_{i,j=1,2} b_{ij} m_{ij}^2 \right).$$

Therefore, $\mathcal{A} = \{(s, q_{ij}) : (s, q_{ij}) \text{ satisfies (2.21)}\}.$

Proof. Note that

$$\begin{aligned} m_{13}^2 &= 1 - m_{11}^2 - m_{12}^2 \geq 0, \\ m_{23}^2 &= 1 - m_{21}^2 - m_{22}^2 \geq 0, \\ m_{31}^2 &= 1 - m_{11}^2 - m_{21}^2 \geq 0, \\ m_{32}^2 &= 1 - m_{12}^2 - m_{22}^2 \geq 0, \\ m_{33}^2 &= m_{11}^2 + m_{12}^2 + m_{21}^2 + m_{22}^2 - 1 \geq 0, \end{aligned}$$

and that for $i, j = 1, 2, 3$, the measure of the set $\{P : m_{ij} = 0\}$ is zero. Thus the inequalities about only q_{ij} in (2.21) are obtained. The inequality about s in (2.21) comes from $(\int d\nu f m_{11})^2 \leq \int d\nu f m_{11}^2$, and the equality holds only if $f m_{11} = \lambda f$ holds for a constant λ , which implies that $f = 0$ for $m_{11} \neq \lambda$. Again we note that the measure of the set $\{P : m_{11} = \lambda\}$ is zero.

The uniqueness of f is deduced immediately from the strict convexity of $f \log f$ about f . To prove the existence, consider the function

$$J(b_1, b_{ij}) = \int d\nu \exp \left(b_1(m_{11} - s) + \sum_{i,j=1,2} b_{ij}(m_{ij}^2 - q_{ij}) \right). \quad (\text{B.1})$$

A stationary point of J satisfies $\partial J / \partial b_1 = \partial J / \partial b_{ij} = 0$, which yields

$$s = \frac{1}{Z} \int d\nu \exp \left(b_1 m_{11} + \sum_{i,j=1,2} b_{ij} m_{ij}^2 \right) m_{11},$$

$$q_{ij} = \frac{1}{Z} \int d\nu \exp \left(b_1 m_{11} + \sum_{i,j=1,2} b_{ij} m_{ij}^2 \right) m_{ij}^2, \quad i, j = 1, 2.$$

Because of the uniqueness, the stationary point of J solves the minimization problem. We will prove that

$$\lim_{b_1^2 + \sum b_{ij}^2 \rightarrow \infty} J = +\infty. \quad (\text{B.2})$$

Since J is bounded from below, (B.2) indicates the existence of a minimizer.

For (B.2), it is sufficient to prove that for any

$$(b_1, b_{11}, b_{12}, b_{21}, b_{22}) \neq (0, 0, 0, 0, 0),$$

there exists a P such that

$$I(P) = b_1(m_{11} - s) + \sum_{i,j=1,2} b_{ij}(m_{ij}^2 - q_{ij}) > 0.$$

Let

$$P_1 = \begin{pmatrix} 1 & 0 & 0 \\ 0 & 0 & 1 \\ 0 & -1 & 0 \end{pmatrix}, \quad P_2 = \begin{pmatrix} -1 & 0 & 0 \\ 0 & 0 & 1 \\ 0 & 1 & 0 \end{pmatrix}, \quad P_3 = \begin{pmatrix} 1 & 0 & 0 \\ 0 & 1 & 0 \\ 0 & 0 & 1 \end{pmatrix}, \quad P_4 = \begin{pmatrix} -1 & 0 & 0 \\ 0 & 1 & 0 \\ 0 & 0 & -1 \end{pmatrix},$$

$$P_5 = \begin{pmatrix} 0 & 1 & 0 \\ 0 & 0 & 1 \\ 1 & 0 & 0 \end{pmatrix}, \quad P_6 = \begin{pmatrix} 0 & 0 & 1 \\ 1 & 0 & 0 \\ 0 & 1 & 0 \end{pmatrix}, \quad P_7 = \begin{pmatrix} 0 & 0 & -1 \\ 0 & 1 & 0 \\ 1 & 0 & 0 \end{pmatrix}, \quad P_8 = \begin{pmatrix} 0 & 1 & 0 \\ 1 & 0 & 0 \\ 0 & 0 & -1 \end{pmatrix}.$$

It is straightforward to verify that

$$\lambda_i I(P_i) = 0$$

holds for arbitrary (b_1, b_{ij}) where

$$\begin{aligned} \lambda_1 &= (\lambda - q_{22}) \left(\frac{1}{2} + \frac{s}{2q_{11}} \right), & \lambda_2 &= (\lambda - q_{22}) \left(\frac{1}{2} - \frac{s}{2q_{11}} \right), \\ \lambda_3 &= (q_{11} + q_{22} - \lambda) \left(\frac{1}{2} + \frac{s}{2q_{11}} \right), & \lambda_4 &= (q_{11} + q_{22} - \lambda) \left(\frac{1}{2} - \frac{s}{2q_{11}} \right), \\ \lambda_5 &= 1 - \lambda - q_{12}, & \lambda_6 &= 1 - \lambda - q_{21}, \end{aligned}$$

$$\lambda_7 = \lambda - q_{11},$$

$$\lambda_8 = q_{12} + q_{21} - (1 - \lambda).$$

Here λ is a real number to be determined. We choose a λ such that $\lambda_i > 0$. It is equivalent to

$$\lambda - q_{22}, q_{11} + q_{22} - \lambda, \lambda - q_{11}, 1 - \lambda - q_{12}, 1 - \lambda - q_{21}, q_{21} + q_{12} - (1 - \lambda) > 0,$$

which yields

$$\max\{q_{11}, q_{22}, 1 - q_{12} - q_{21}\} < \lambda < \min\{1 - q_{12}, 1 - q_{21}, q_{11} + q_{22}\}.$$

From the constraints on q_{ij} , the upper bound is greater than the lower bound, which guarantees the existence of λ . Note that

$$\sum_{i=1}^8 \lambda_i = 1.$$

Let

$$A = b_1 s + \sum_{i,j=1,2} b_{ij} q_{ij}.$$

We claim that $I(P_i) > 0$ for some i . Otherwise $I(P_i) = 0$ for every i . Expanding these equalities, we have

$$\pm b_1 + b_{11} = \pm b_1 + b_{11} + b_{22} = b_{21} = b_{12} = b_{22} = b_{12} + b_{21} = A.$$

It is easy to deduce that $b_1 = b_{ij} = 0$. □

B.2 Some equalities

The derivatives of $F_{entropy}$ about the tensors are

$$\frac{1}{k_B T} \frac{\partial F_{entropy}}{\partial (\mathbf{p}, Q_1, Q_2)} = (\mathbf{b}, B_1, B_2). \quad (\text{B.3})$$

We prove it for \mathbf{p} as an example. Note that

$$\frac{\partial \log Z}{\partial (\mathbf{b}, B_1, B_2)} = \frac{1}{Z} \frac{\partial Z}{\partial (\mathbf{b}, B_1, B_2)} = (\mathbf{p}, Q_1, Q_2). \quad (\text{B.4})$$

Hence

$$\begin{aligned} & \frac{1}{k_B T} \frac{\partial F_{entropy}}{\partial \mathbf{p}} \\ &= \frac{\partial (\mathbf{b} \cdot \mathbf{p} + B_1 : Q_1 + B_2 : Q_2 - \log Z)}{\partial \mathbf{p}} \\ &= \mathbf{b} + \mathbf{p} \cdot \frac{\partial \mathbf{b}}{\partial \mathbf{p}} + Q_1 : \frac{\partial B_1}{\partial \mathbf{p}} + Q_2 : \frac{\partial B_2}{\partial \mathbf{p}} - \frac{\partial \log Z}{\partial \mathbf{p}} \\ &= \mathbf{b} + \frac{\partial \log Z}{\partial \mathbf{b}} \cdot \frac{\partial \mathbf{b}}{\partial \mathbf{p}} + \frac{\partial \log Z}{\partial B_1} : \frac{\partial B_1}{\partial \mathbf{p}} + \frac{\partial \log Z}{\partial B_2} : \frac{\partial B_2}{\partial \mathbf{p}} - \frac{\partial \log Z}{\partial \mathbf{p}} \\ &= \mathbf{b} + \frac{\partial \log Z}{\partial (\mathbf{b}, B_1, B_2)} \cdot \frac{\partial (\mathbf{b}, B_1, B_2)}{\partial \mathbf{p}} - \frac{\partial \log Z}{\partial \mathbf{p}} \end{aligned}$$

$$=\mathbf{b}.$$

The derivatives of F about $b_{ij}(x)$ can be written as

$$\frac{\partial F}{\partial b_{ij}(x)} = \frac{\partial q_{kl}(x)}{\partial b_{ij}(x)} \frac{\partial F}{\partial q_{kl}(x)}. \quad (\text{B.5})$$

And note that

$$\frac{\partial q_{kl}(x)}{\partial b_{ij}(x)} = \frac{\partial^2 Z}{\partial b_{ij}(x) \partial b_{kl}(x)} = \langle (m_{11}, m_{11}^2, m_{12}^2, m_{21}^2, m_{22}^2)^T (m_{11}, m_{11}^2, m_{12}^2, m_{21}^2, m_{22}^2) \rangle.$$

is positive definite. Thus

$$\left(\frac{\partial F}{\partial b_{ij}(x)} \right)^T \frac{\partial F}{\partial q_{ij}(x)} = \left(\frac{\partial F}{\partial q_{ij}(x)} \right)^T \frac{\partial^2 Z}{\partial b_{ij}(x) \partial b_{kl}(x)} \frac{\partial F}{\partial q_{ij}(x)} > 0. \quad (\text{B.6})$$

Acknowledgments. P. Zhang is partly supported by National Natural Science Foundation of China (Grant No. 11421101 and No. 11421110001).

References

- [1] B. R. Acharya, A. Primak, and S. Kumar. Biaxial nematic phase in bent-core thermotropic mesogens. *Phys. Rev. Lett.*, 92:145506, 2004.
- [2] F. Bisi, E. G. Virga, E. C. Gartland, G. De Matteis, A. M. Sonnet, and G. E. Durand. Universal mean-field phase diagram for biaxial nematics obtained from a minimax principle. *Phys. Rev. E*, 73:051709, 2006.
- [3] V. Borshch, Y.-K. Kim, J. Xiang, M. Gao, A. Jákli, V. P. Panov, J. K. Vij, C. T. Imrie, M. G. Tamba, G. H. Mehl, and O. D. Lavrentovich. Nematic twist-bend phase with nanoscale modulation of molecular orientation. *Nat. Commun.*, 4:2635, 2013.
- [4] P. J. Camp, M. P. Allen, and A. J. Masters. Theory and computer simulation of bent-core molecules. *J. Chem. Phys.*, 111:9871, 1999.
- [5] D. Chen, J. H. Porada, J. B. Hooper, A. Klittnick, Y. Shen, M. R. Tuchband, E. Körblova, D. Bedrov, D. M. Walba, M. A. Glaser, J. E. MacLennan, and N. A. Clark. Chiral heliconical ground state of nanoscale pitch in a nematic liquid crystal of achiral molecular dimers. *Proc. Natl. Acad. Sci. USA*, 110:15931, 2013.
- [6] D. A. Coleman, J. Fernsler, N. Chattham, M. Nataka, Y. Takanishi, E. Körblova, D. R. Link, R.-F. Shao, W. G. Jang, J. E. MacLennan, O. Mondainn-Monval, C. Boyer, W. Weissflog, G. Pelzl, L.-C Chien, J. Zasadzinski, J. Watanabe, D. M. Walba, H. Takezoe, and N. A. Clark. Polarization-modulated smectic liquid crystal phases. *Science*, 301:1204, 2003.
- [7] A. Dewar and P. J. Camp. Dipolar interactions, molecular flexibility, and flexoelectricity in bent-core liquid crystals. *J. Chem. Phys.*, 123:174907, 2005.

- [8] I. Dozov. On the spontaneous symmetry breaking in the mesophases of achiral banana-shaped molecules. *Europhys. Lett.*, 56:247, 2001.
- [9] A. Eremin, A. Nemeş, R. Stannarius, and W. Weissflog. Ambidextrous bend patterns in free-standing polar smectic- CP_F films. *Phys. Rev. E*, 78:061705, 2008.
- [10] C. Greco and A. Ferrarini. Entropy-driven chiral order in a system of achiral bent particles. *Phys. Rev. Lett.*, 115:147805, 2015.
- [11] J. Han, Y. Luo, W. Wang, and P. Zhang. From microscopic theory to macroscopic theory: a systematic study on modeling for liquid crystals. *Arch. Ration. Mech. An.*, 215:741–809, 2015.
- [12] Y. Lansac, P. K. Maiti, N. A. Clark, and M. A. Glaser. Phase behavior of bent-core molecules. *Phys. Rev. E*, 67:011703, 2003.
- [13] V. L. Lorman and B. Mettout. Unconventional mesophases formed by condensed vector waves in a medium of achiral molecules. *Phys. Rev. Lett.*, 82:940, 1999.
- [14] L. A. Madsen, T. J. Dingemans, M. Nakata, and E. T. Samulski. Thermotropic biaxial nematic liquid crystals. *Phys. Rev. Lett.*, 92:145505, 2004.
- [15] J. E. Mayer and M. G. Mayer. *Statistical Mechanics*. John Wiley & Sons, 1940.
- [16] R. B. Mayer. Structural problems in liquid crystal physics. In R. Balian and G. Weil, editors, *Molecular Fluids*, Les Houches Summer School in Theoretical Physics, 1973, pages 273–373. Gordon and Breach, New York, 1976.
- [17] R. Memmer. Liquid crystal phases of achiral banana-shaped molecules: a computer simulation study. *Liq. Cryst.*, 29:483, 2002.
- [18] C. Meyer, G. R. Luckhurst, and I. Dozov. Flexoelectrically driven electroclinic effect in the twist-bend nematic phase of achiral molecules with bent shapes. *Phys. Rev. Lett.*, 111:067801, 2013.
- [19] N. Vaupotič, M. Čepič, M. A. Osipov, and E. Gorecka. Flexoelectricity in chiral nematic liquid crystals as a driving mechanism for the twist-bend and splay-bend modulated phases. *Phys. Rev. E*, 89:030501, 2014.
- [20] T. D. Nguyen, Z. Zhang, and S. C. Glotzer. Molecular simulation study of self-assembly of tethered v-shaped nanoparticles. *J. Chem. Phys.*, 129:244903, 2008.
- [21] V. P. Panov, M. Nagaraj, J. K. Vij, Yu. P. Panarin, A. Kohlmeier, M. G. Tamba, R. A. Lewis, and G. H. Mehl. Spontaneous periodic deformations in nonchiral planar-aligned bimesogens with a nematic-nematic transition and a negative elastic constant. *Phys. Rev. Lett.*, 105:167801, 2010.
- [22] G. Pelzl, A. Eremin, S. Diele, H. Kresse, and W. Weissflog. Spontaneous chiral ordering in the nematic phase of an achiral banana-shaped compound. *J. Mater. Chem.*, 12:2591–2593, 2002.

- [23] S. M. Shamid, D. W. Allender, and J. V. Selinger. Predicting a polar analog of chiral blue phases in liquid crystals. *Phys. Rev. Lett.*, 113:237801, 2014.
- [24] S. M. Shamid, S. Dhakal, and J. V. Selinger. Statistical mechanics of bend flexoelectricity and the twist-bend phase in bent-core liquid crystals. *Phys. Rev. E*, 87:052503, 2013.
- [25] H. Takezoe and Y. Takanishi. Bent-core liquid crystals: their mysterious and attractive world. *Jpn. J. Appl. Phys.*, 45:597, 2006.
- [26] E. G. Virga. Double-well elastic theory for twist-bend nematic phases. *Phys. Rev. E*, 89:052502, 2014.
- [27] J. Xu and P. Zhang. *preprint*.
- [28] J. Xu and P. Zhang. From microscopic theory to macroscopic theory — symmetries and order parameters of rigid molecules. *Sci. China. Math.*, 57:443, 2014.
- [29] J. Xu and P. Zhang. The transmission of symmetry in liquid crystals. *To appear in Comm. Math. Sci.*, 2016.